Journal of Materials Chemistry A

Facile Preparation Method of Surface Patterned Polymer Electrolyte Membranes for Fuel Cell Applications

Journal:	*Journal of Materials Chemistry A*
Manuscript ID:	TA-ART-02-2014-000674.R1
Article Type:	Paper
Date Submitted by the Author:	05-Mar-2014

Complete List of Authors:	Koh, Jong Kwan; Yonsei University, Department of Chemical and Biomolecular Engineering Jeon, Yukwon; Yonsei University, Department of Chemical and Biomolecular Engineering Cho, Yong il; Yonsei University, Department of Chemical and Biomolecular Engineering Kim, Jong Hak; Yonsei University, Department of Chemical and Biomolecular Engineering Shul, Yong-Gun; Yonsei University, Department of Chemical and Biomolecular Engineering

Journal of Materials Chemistry A RSCPublishing

ARTICLE

Facile Preparation Method of Surface patterned Polymer Electrolyte Membranes for Fuel Cell Applications

Cite this: DOI: 10.1039/x0xx00000x

Received ooth January 2012,
Accepted ooth January 2012

DOI: 10.1039/x0xx00000x

www.rsc.org/

Jong Kwan Koh[‡], Yukwon Jeon[‡], Yong il Cho, Jong Hak Kim[*], Yong Gun Shul[*]

We report a facile patterning method that facilitates production of large-area platforms with well-arrayed micro/nanopatterns of polymer electrolyte membrane (PEM) at low cost using an elastomeric mold at room temperature without hot-pressing. Membrane/electrode interfacial properties on the cathode side are controlled by the patterned structure of the membrane, which in turn directly affects the electrochemically active surface area (ECSA) and Pt utilization of the catalyst. This confirmed electrochemical property improves the performance of membrane electrode assembly (MEA). A MEA fabricated with 3 × 5 μm (width × gap) micropatterned Nafion membrane exhibits a current density of 1.79 A/cm^{-2} at 0.6 V and a power density of 1.26 W/cm^2 at 75°C; these values are 53% and 59% greater than those of the corresponding MEA without a patterned membrane, respectively, and are among the highest performances reported for polymer electrolyte membrane fuel cells (PEMFCs). However, use of a nanopatterned membrane decreases performance due to insufficient infiltration of ionomer into the grooved surface, leading to poor mechanical/electrical contact between the membrane and the electrode. Membrane morphology and the structure of the membrane/electrode interface are characterized by field emission scanning electron microscopy (FE-SEM), cyclic voltammetry (CV), and impedance spectroscopy.

Introduction

Fuel cells are 'green' electrochemical devices that convert chemical energy directly into electrical energy. Among fuel cells, polymer electrolyte membrane fuel cells (PEMFCs) have great potential as a source of clean energy for transportable, stationary, and portable power applications due to their high energy conversion efficiencies and low operating temperatures.[1-9] Extensive research and development of membrane electrode assemblies (MEAs) have resulted in the commercial application of PEMFC technology.[10-13] However, there remain several challenges for commercialization of PEMFCs such as the high cost, low durability, reliability and limited lifespan of MEAs. The most common approach that has been taken to tackle these issues is to use a high surface area and electronic conducting carbon materials such as carbon black, carbon fiber, mesoporous carbon, and carbon nanotubes to improve electrochemical activity and utilization of catalyst.[14-18] Another approach is control of interfacial contact between the electrode and the polymer electrolyte membrane (PEM) to improve the surface area of the MEA.

Patterning is a well-known method for constructing large active areas and periodic photonic structures, and thus has received tremendous attention as a means of boosting light harvesting efficiency in solar cells.[19,20] In PEMFC applications, the patterned structure shows also an improvement in the electrochemical property and fuel cell performance. M. Aizawa et al.[21] reported that the use of a patterned PEM can provide proton transport through the patterns with a better interfacial contact between the electrode and the PEM, leading to increased electrochemical surface area a wide cathode catalyst region and reaction rate. Moreover, the oxygen permeates by shorter distances through the catalyst layer to react with the transported proton. In addition, a better water management is reported from the operation at a dehydration conditions.[22] Although some MEAs have been fabricated with surface-modified structural PEM,[21-30] such a facile patterning method at low temperature without hot pressing has not been reported. For example, structural PEMs have been prepared using thermal imprint lithography,[24] and imprinting method with a patterned silicon mold under high pressure/temperature (over 150 °C) conditions.[21-22, 26-28] However, the high temperature could have an influence to the polymer membranes. Some of the preparation methods are porous polytetrafluoroethylene (PTFE) template,[23-25] electron beam[29-30] and a plasma etching methods.[31-32] Rather, expensive and complicated fabrication processes that are difficult to use for mass production are employed to increase the interfacial contact between the electrode/membrane.

Incorporation of a patterned PEM on the cathode side can produce a uniform distribution of catalyst nanoparticles, such as Pt. It could also directly affect the utilization of metal catalyst, because catalytic effects in MEAs are generated by a surface phenomenon.[33-36] Utilization of metal catalysts is strongly related to metal dispersion and the amount of metal atoms exposed, which are in turn correlated with the size of the metal in nanometers. Pt utilization for commercial Pt/C in PEMFC applications is in the range of 25-50% when the Pt particle size ranges from 2-4 nm.[37-41] Basically, effective design of a MEA can improve the electrochemical surface area and metal

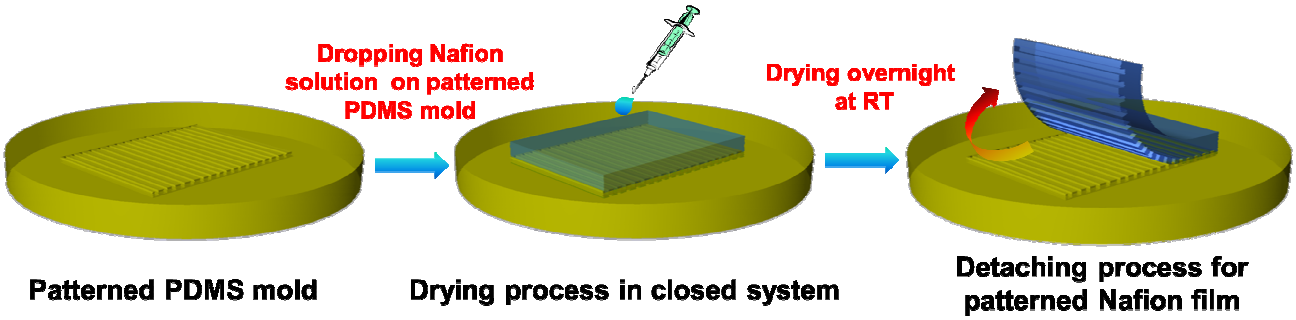

Scheme 1. A schematic of the fabrication process of Nafion membranes with patterned structures. (Left) Schematic image of the PDMS mold, (middle) casting process for preparation of a patterned Nafion membrane from a 5 wt% solution, (right) detachment of the dried Nafion membrane from the PDMS mold. See the text for detailed process conditions.

utilization in the MEA, facilitating the transport of protons and mass transfer of reactants. A MEA with a large electrochemical surface area would have a high current carrying capacity, and thus high efficiency when used in PEMFCs.

Here, we report a patterning method that allows facile production of a large-area platform with well-arrayed patterns of PEM without hot-pressing at low cost using readily available solutions and elastomeric nano/micro-structured molds. The fabrication process using PDMS mold not a stamp was available to control the thickness of the film and make patterned surface with large area. With many PDMS molds, it could be possible to produce many patterned Nafion film in a short time, repeatedly. Besides, only one silicon master was needed during fabrication period. This polymer molding approach enhances contact at the membrane/electrode interface, thereby improving catalyst utilization and increasing the electrochemical surface area (ECSA) and the electrochemical activity on the cathode side of the PEMFC. In particular, we investigated the effect of pattern size on membrane surface area, Pt mean particle size, and Pt utilization in detail to understand the effect of the pattern structure to the catalytic reaction. We also report current density-voltage (I-V) curves, ohmic resistance, and charge transfer resistance of MEAs with various membrane line patterns.

Results and discussion

Preparation of patterned membranes

The fast and simple procedure even at room temperature that we developed to fabricate patterned Nafion membranes using elastomeric polydimethylsiloxane (PDMS) mold is illustrated in Scheme 1. The patterned PDMS was not used as a stamp but as a mold for surface pattern of nafion film. Patterned PDMS molds were prepared using a 0.5 mm-thick patterned silicon master (the thickness of the silicon wafer itself). Nafion solution was poured onto the patterned PDMS mold surfaces. Because the size of the pattern on the PDMS is too small, we needed to use the 5 wt% Nafion thin solution in a mixture of lower aliphatic alcohols and water for penetration into the few micro-patterns. We casted the same amount of Nation thin solution on the same area of the patterned PDMS, which means same thickness of the Nafion were created on the PMDS surface. After complete drying at room temperature overnight, the patterned Nafion films were carefully detached from the PDMS molds and kept at room temperature. The fabrication process using PDMS mold showed many advantages during the procedure of Nafion film with patterned surface. At first, we can control the thickness of the film and make patterned surface with large area. Second, if we have many PDMS molds, you can produce many patterned Nafion film in a short time, repeatedly. In addition, it was possible to produce the same membranes as many as we want by using only one silicon master, indicating good reproducibility and processibility. In this work, each patterned membranes were prepared at least five times without any degradation in the molds as well as the polymer membranes. These PDMS molds can be reused without any washing or other additional treatments, which is an additional advantage for industrial applications.

Nafion membranes fabricated using the elastomeric PDMS molds showed a uniform thickness of approximately 50 μm with good mechanical properties, being strong enough and not brittle to apply it to the MEA. We can confirm the steady materializing of the

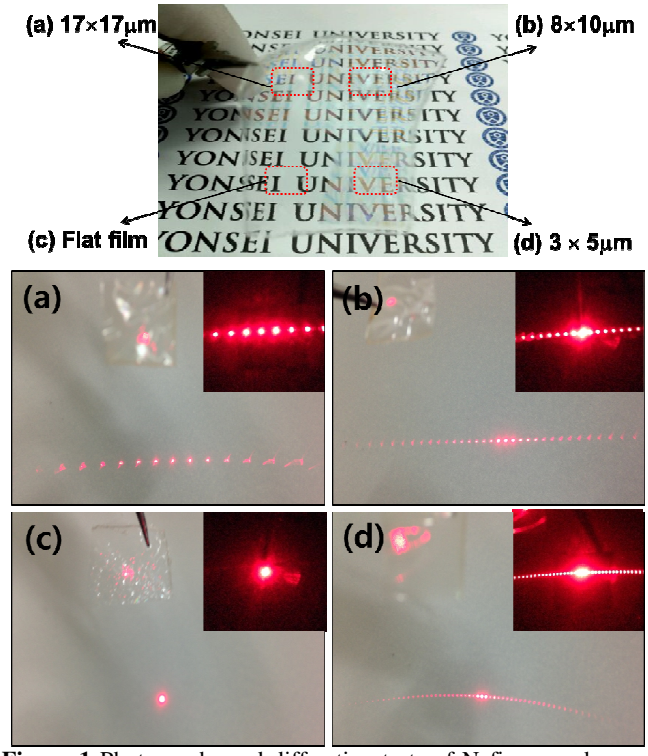

Figure 1 Photographs and diffraction tests of Nafion membranes with four types of line-patterned structures: (a) 17×17 μm, (b) 8×10 μm, (c) flat, and (d) 3×5 μm line patterns.

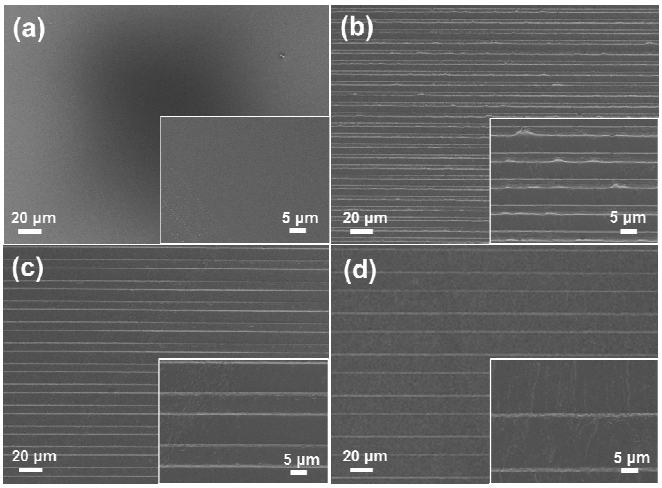

Figure 2 FE-SEM surface images of Nafion membranes with different pattern sizes (pattern size × period of pattern): (a) flat film, (b), PM1 (3×5 μm), (c) PM2 (8×10 μm), (d) PM3 (17×20 μm). Insets are magnified images of each sample.

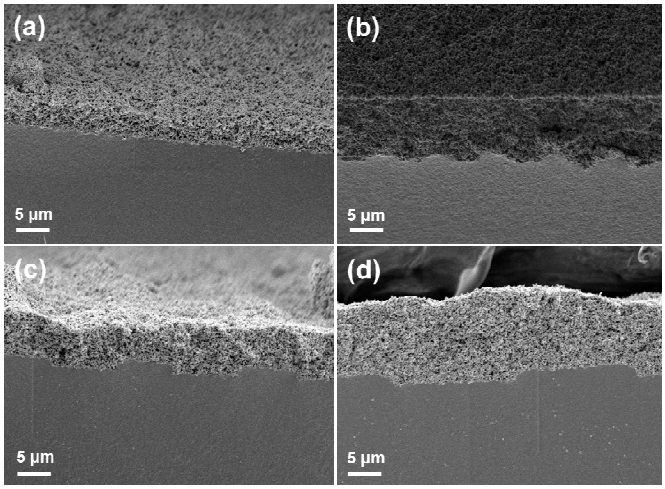

Figure 4 FE-SEM cross-sectional images of the interface between the catalyst layer and Nafion membranes with different pattern sizes (pattern size period of pattern): (a) flat film, (b), PM1 (3×5 μm), (c) PM2 (8×10 μm), (d) PM3 (17×20 μm).

film thickness empirically and observed the thickness of the film by means of SEM, repeatedly. There was not any thickness deduction due to the repeated casting of Nafion solution. Different levels of transparency and reflection along with anticipated patterns were observed depending on the pattern structure, as shown in Figure 1. Detailed surface morphologies of the Nafion membranes were characterized by scanning electron microscopy (SEM). As shown in Figure 2, all micro-sized patterns on the Nafion surfaces were clearly distinguishable with a well-defined line width along the PDMS molds; no defects were observed. Nafion membranes with various patterned structures such as circular, rectangular, and hexagonal shapes can be also prepared, as shown in Figure S1, indicating that this is a versatile universal method for constructing patterned membranes.

To evaluate MEA performance, the following Nafion membranes with different line patterns were prepared by varying the width × gap dimensions as follows: 3 × 5 μm, patterned membrane 1 (PM1); 8 × 10 μm, patterned membrane 2 (PM2); 17 × 20 μm, patterned membrane 3 (PM3); and 250 × 350 nm, nanopatterned membrane (NPM). Specific membrane surface areas were calculated for the fuel cell active area of 1 cm^2, as shown in Table 1. Compared to the flat membrane without a pattern, the specific surface area of PM1, PM2, and PM3 increased by 18.8%, 8.3%, and 4.4%, respectively. Figure 3 shows cross-sectional SEM images of the patterned membranes. The height of all patterns was precisely controlled at approximately 1.5 μm, and thus the total membrane thickness was approximately 50±1 μm (Table 1), indicating that membrane thickness had a negligible effect on pattern height.

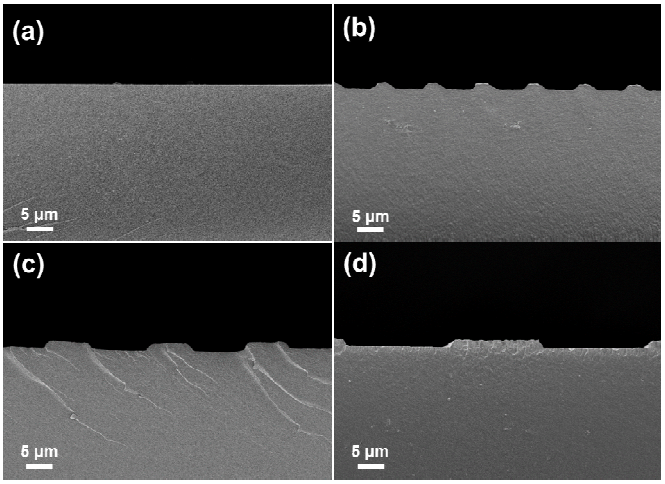

Figure 3 FE-SEM cross-sectional images of Nafion membranes with different pattern sizes (the depth of each pattern was approximately 1.5 μm): (a) flat film (film thickness: 51.7 μm), (b) PM1 (48.3 μm), (c) PM2 (51.3 μm), (d) PM3 (50.1 μm).

For PEM fuel cell application, a catalyst layer was sprayed directly on the cathode side of the Nafion membranes. Figure 4 shows cross-sectional images of the membrane/catalyst layer interface of each prepared MEA, in which the catalyst layers are strongly attached to the membrane surface. The original patterned structures of the membranes were not significantly perturbed at the interface despite deep coverage by the thick catalyst layer. Line protrusion at the cathode side would increase the area of intersection with the catalyst layer, resulting in an increase in membrane surface area, electro-catalytic activity, and electron/proton transfer pathways. Furthermore, a patterned surface could reduce the amount of catalyst required, thereby reducing the cost of the fuel cell stack dramatically.[21-25]

Patterned membranes increase the active area of MEAs

We characterized the electrochemical properties of the catalyst layers in the MEAs by cyclic voltammetry (CV) measurements as shown in Figure 5a. Typical CV curves with strong hydrogen adsorption/desorption peaks were observed without any vertical shifts, irrespective of the patterned structures. Magnified plots revealed a significant increase in the hydrogen adsorption peak intensity, indicating larger peak areas in the MEAs with micropatterned Nafion membranes. This is direct evidence that the catalytic properties of the MEAs were enhanced by the patterned structures, most likely because the catalyst layer could receive the reactants easily, resulting in efficient reactions at the catalyst surface.

An important determinant of the electrochemical properties of PEMFCs is the electrochemical active surface area

(ECSA) of the catalyst Pt nanoparticles located on the exterior electrode surface. Protons transport through the patterns can react with oxygen which permeates with shorter distances through the catalyst layer that the ORR occurs in a wider cathode catalyst region. Therefore, this structure is contributed to the reaction for the MEA performance. That is why ECSA is important to prove the effect of the patterned structure. ECSA values can be calculated from the hydrogen adsorption charge on the smooth Pt surface by integrating the hydrogen adsorption peak from the CV profile after correction for double layer capacitance. We used the following equation to calculate the ECSA (m^2/g) values of the Pt/C electrocatalyst on the cathode side of the MEAs:[33-36]

$$ECSA = \frac{100 \cdot Q_H}{\Gamma \cdot L} \quad (1)$$

where Q_H is the electrooxidation charge of the adsorbed hydrogen on the Pt surface integrated from the hydrogen adsorption peak, Γ is the electrical charge associated with monolayer adsorption of the hydrogen on the Pt catalyst surface (generally 21 mC/cm^2), and L is the Pt mass in the cathode (mg). ECSA is considered a good indicator of the quality of the catalyst layer in a MEA because it reflects particle location, particle size, and size distribution. As shown in Figure 5b and Table 1, the ECSA values of PM1, PM2, PM3 with micropatterned structures were 58.2, 51.2 and 45.2 m^2/g, respectively; all these values are much higher than that of NPM (32.6 m^2/g), indicating that micropatterning was more effective than nanopatterning at increasing ECSA. Furthermore, the ECSA values of all micropatterned MEAs were higher than that of the flat MEA without patterning (40.0 m^2/g). The highest value was obtained for the PM1-based MEA; the triple phase boundary at the interface resulted in highest utilization of the Pt catalyst.

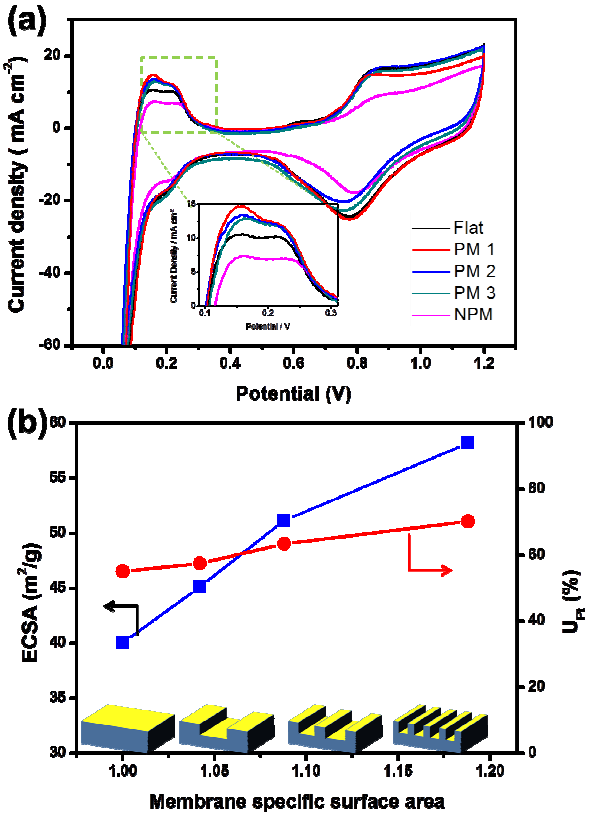

Figure 5 (a) CV curves of single MEAs fabricated with flat and micro/nanopatterned Nafion membranes (inset: magnified regions for hydrogen adsorption charges), (b) ECSAs and Pt utilization of the catalyst layer as a function of membrane specific surface areas, calculated from the hydrogen adsorption charge on the smooth Pt surface by integration of the CV profile.

Calculation of Pt utilization (U_{Pt}) is considered a good way to better understand catalytic behavior and interface conditions in MEAs. The utilization percentage of Pt can be obtained from the CV measurements taking Pt particle size into account. The particle size of the Pt catalyst is also an important determinant of catalyst behavior because electrochemical reactions take place at the effective surface area of the Pt particles. Assuming that each Pt nanoparticle had a uniform spherical shape, we calculated the surface area of Pt (S_{Pt}) using equation 2:[35]

$$S_{Pt} = \frac{\text{surface}}{\text{mass}} = \frac{\pi \cdot D^2}{\pi D^3 / 6} = \frac{6}{\rho \cdot D} \quad (2)$$

where ρ is the mass density of Pt (21.4 g/cm^3) and D is the mean particle size of Pt calculated from XRD patterns (Figure S2) of each catalyst layer in the cathode. As summarized in Table 1, mean particle sizes were in the typical range of 3-4 nm for all MEAs when calculated using Scherrer's equation with a shape constant (K) of 0.9 on the Pt (111) diffraction peak. A slight difference in the XRD peak intensity between the patterned membrane and flat membrane was observed maybe due to the change in the diffraction angle through a rough surface of the catalyst layers by spraying catalyst ink directly to the patterned surface of the Nafion membrane.

Utilization of Pt catalyst (U_{Pt}) can be estimated from the ratio of ECSA to the calculated S_{Pt}, which expresses the amount of active surface Pt atoms for electrochemical reactions, as shown in equation 3.[37-39]

$$U_{Pt} = \frac{ECSA}{S_{Pt}} \quad (3)$$

The U_{Pt} values for PM1-, PM2-, and PM3-based MEAs were 70.2%, 63.5%, and 57.5%; all these values are larger than that of the flat MEA without a pattern (55.1%), indicating that the patterned structure increased utilization of the Pt catalyst. However, the U_{Pt} value of the NPM-based MEA (42.6 %) was unexpectedly smaller than that of the flat MEA, indicating that the nanopatterned structure was not effective at improving the interfacial area of the membrane/electrode. As shown in Figure 5b, utilization of Pt increased as ECSA increased, as the latter parameter is proportionally related to the specific surface area of the membrane. This suggests that a patterned structure with a higher surface area facilitates efficient distribution of Pt nanoparticles in the active contact zone for electric and proton pathways. Addition of a micropatterned structure to Nafion membranes is therefore likely to enhance the electrochemical performance of MEAs due to high Pt utilization and a high active surface area.

PEMFC performance

Polarization curves (I-V) of the single cell performance of MEAs fabricated with unpatterned and variously patterned Nafion membranes are shown in Figure 6a. The open-circuit voltage of all MEAs was the same at 0.98 V, confirming fabrication of MEAs with a similar membrane thickness that do not affected the conductivity with no gas crossover. At the voltage of 0.6 V, the current density of the PM1-, PM2-, and PM3-based MEAs was 1.79 A/cm^2, 1.35 A/cm^2, and 1.29 A/cm^2, respectively, which are all greater than that of the flat MEA without patterning (1.17 A/cm^2), indicating that a micropatterned structure improves PEMFC performance. In particular, the current density of the PM1-based MEA was 52.9% greater than that of the flat MEA. This micropatterned membrane may also be extended to the anode side for further performance, but we mainly focused on the catalytic reaction. As described above, the increased performances of the micropatterned MEAs were due to improved interfacial properties at the electrode/membrane, leading to an increase in the electrochemically active surface area and better Pt utilization at the cathode. The gradual nature of the I-V slopes in the low voltage range should also be noted. In general, this region reflects performance associated with the interfacial design of the MEA, in particular the triple phase boundary.[39] High current densities in the low voltage region were obtained for the micropatterned MEAs, which is further evidence that the micropatterned structures enhanced the proton and electron pathways through three-dimensional pore structures, resulting in effective mass transfer of reactants and products. A significant increase in power density was obtained for the micropatterned MEAs versus the non-patterned MEA, as shown in Figure 6b, and this was correlated with an increase in current density. The maximum power density of the PM1-based MEA was 1.26 W/cm^2, which is one of the highest values reported for PEMFCs[1-10, 21-32] and is high enough for practical application of this MEA in PEMFCs. The current density at 0.6 V and the maximum power density of PM1-based MEA were even greater than those of MEA with the commercial Nafion 212 membrane, as shown in Figure S3 and Table S1. It should be noted that all the MEAs were fabricated without hot-pressing, which is advantageous in terms of energy saving.

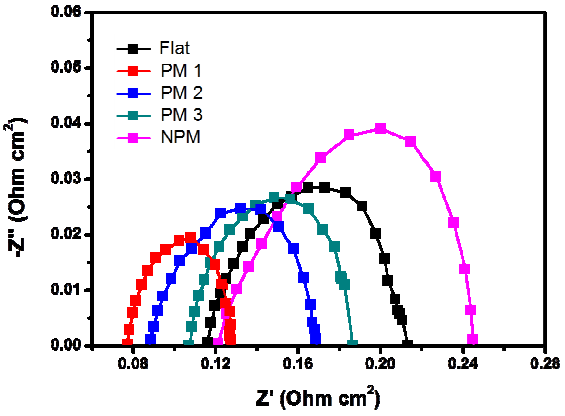

Figure 7 Nyquist plots of single MEAs fabricated with flat and patterned Nafion membranes.

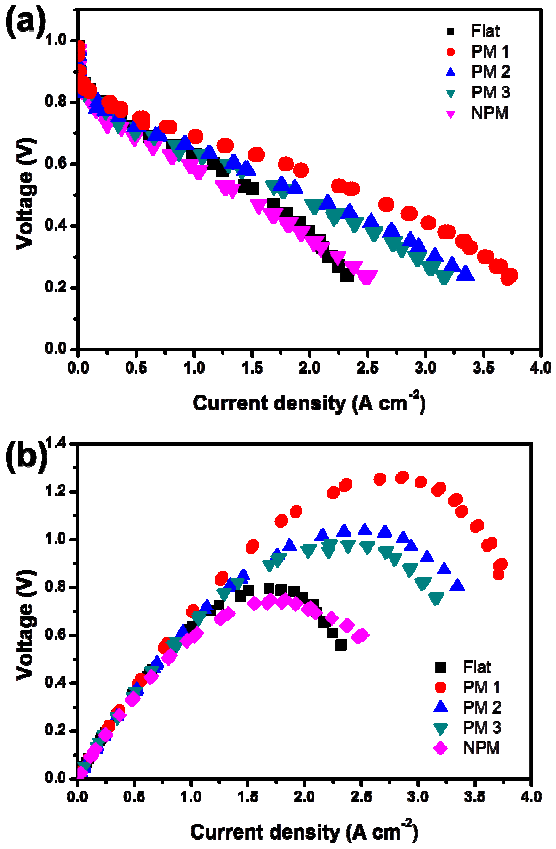

Figure 6 (a) polarization (I-V) curves and (b) power density curves of single PEM fuel cells with flat and micro/nanopatterned membranes at 75°C and 100% RH.

Table 1. Membranes characteristics and electrochemical properties of MEAs fabricated using patterned membranes.

	Flat	PM1	PM2	PM3	NPM
Pattern size[a]	-	3/5 /1.5	8/10 /1.5	17/20/ 1.5	0.25/0.35/ 0.15
Specific surface area	1	1.19	1.08	1.04	1.22
Thickness (μm)	50.7	50.3	50.5	50.1	49.1
Q_H (mC)	33.6	48.9	43.0	37.9	27.5
ECSA (m^2/g)	40.0	58.2	51.2	45.1	32.6
Pt mean particle size (nm)	3.86	3.38	3.48	3.57	3.67
S_{Pt} (m^2/g)	72.7	82.9	80.6	78.5	76.5
U_{Pt} (%)	55.1	70.2	63.5	57.5	42.6
Current density[b]	1.17	1.79	1.35	1.29	0.97
Maximum power density[c]	0.79	1.26	1.04	0.98	0.75
Ohmic resistance[d]	0.12	0.08	0.09	0.11	0.12
Charge transfer resistance[d]	0.10	0.05	0.08	0.08	0.12

[a](μm), (width/space/height), [b]at 0.6 V (A/cm^2), [c](W/cm^2), [d](Ω cm^2)

To characterize membrane resistance and interfacial resistance at the electrode/membrane, Nyquist plots of electrochemical impedance spectroscopy (EIS) were generated and are shown in Figure 7. Nyquist plots show semi-circles with ohmic resistance at the intercept with the x-axis at a high frequency, which is generally taken as the membrane (ohmic) resistance. Charge transfer resistance at the interface of the electrode/membrane was obtained from the intercept with the x-axis at a low frequency, which is related to oxygen reduction reactions. Ohmic loss is mainly related to the thickness of the membrane and defects in the membrane. MEAs with patterned structures had a smaller ohmic resistance than the flat MEA without a pattern. For example, the ohmic resistance of the PM1-based MEA (0.08 Ω cm^2) was somewhat smaller than that of the flat MEA (0.12 Ω cm^2), despite very similar membrane thicknesses. The pattern depths of the membranes were all 1.5 μm, which could have a membrane thinning effect. Furthermore, the decrease in resistance might be due to the facile transport of ions through the line patterns. Changes in the charge transfer resistances, governed by ionic conductivity and electrode/membrane interface resistance, were also confirmed by EIS analysis. As shown in Figure 7 and Table 1, the micropatterned MEAs demonstrated a substantial decrease in charge transfer resistance from 0.10 Ω cm^2 to 0.05, 0.08, and 0.08 Ω cm^2 for PM1, PM2, and PM3, respectively. The PM1-based MEA had particularly the lowest resistance of the MEAs in both ohmic and charge transfer resistances due to its highest specific area through line-patterning among the MEAs fabricated, yielding the highest performance MEA.

We also fabricated a MEA with a nanopatterned membrane (NPM) with dimensions of 250 nm × 350 nm × 150 nm (width × space × height); we hypothesized that this MEA would show the best PEMFC performance among the MEAs because of the greater surface area of the nanopattern than the micropatterns (Table 1). Unexpectedly, the MEA with a nanopattern performed poorly, i.e. a current density of 0.97 A/cm^2 at 0.6 V and a power density of 0.97 W/cm^2; these values are even lower than that of the flat MEA without a pattern. This may be due to insufficient infiltration of Pt/C/Nafion hybrid into the grooved surfaces due to size mismatch between the nanopatterned groove and the hybrid, resulting in a decrease in interfacial area and thus poor adhesion of the electrode/membrane. Nafion, which we used as an ionomer for MEA fabrication, is typically dispersed as a micelle in a mixture of lower aliphatic alcohols and water using a surfactant. Previous studies have shown that the size of a well-dispersed Pt/C/Nafion hybrid is typically bimodal with a majority of small aggregates of 0.023 – 0.275 μm in size and a minority of larger aggregates in the size range of 1 – 10 μm. [40, 41] The size of the nanopatterned groove was smaller than that of Pt/C/Nafion hybrid, which may have been responsible for the large increase in ohmic resistance and charge transfer resistance observed for the NPM-based MEA. We conclude, therefore, that pattern size should be carefully designed to control the interface between the membrane and the catalyst layer. Our patterning approach can be used to increase bonding between the membrane and the electrode, which may mitigate degradation mechanisms, such as delamination, caused by operating cycles.

Experimental

PDMS mold fabrication

For PDMS mold fabrication, 20 vol% dilute prepolymer in hexane and curing agent (Dow Corning, Sylgard-184) were mixed at a 10:1 weight ratio, followed by degassing for 1 h. To prevent the cured PDMS from sticking, silicon master (29 mm × 24.2 mm, period: 606 nm, groove depth: 190 nm; SNS-C16.5-2924-190-P, LightSmyth Technologies Inc., USA) was placed in a Petri dish with a few drops of tridecafluoro-1,1,2,2-tetrahydrooctyl-1-trichlorosilane (TFPCS) and then in a desiccator connected to a vacuum line for 30 min. After deposition of a hydrophobic monolayer onto the silicon master, the thermal curable liquid mixture was poured into a master mold placed in a Petri dish. Then, the bubbles and hexane were removed in a closed system through a hole in the aluminum foil for 24 hours. The Petri dish containing both the master and PDMS prepolymer was placed in an oven at 80ºC for 3 h, and the cured PDMS was peeled off and carefully separated from the Petri dish and master. PDMS molds with various patterned structures were cut to the desired size for patterning Nafion membranes.

Patterning Nafion membranes

Nafion® solution (5 wt.% solution in lower aliphatic alcohol/H_2O mix, EW = 1100, Aldrich) was poured onto the patterned PDMS mold surface. After complete drying at room temperature for 12 h, patterned Nafion films with a thickness of 50 ± 2 μm were obtained. Nafion films with large and differently patterned structures were prepared using various patterned replica PDMS molds without any further treatment. To investigate the pattern effect, a flat Nafion film was also produced by using a PDMS mold without patterns. We prepared casted Nafion thin film at least 5 times for each, which were all strong enough to measure of it and fabricate the MEAs. The morphologies of the patterned membranes were determined by high resolution SEM (Carl Zeiss, model SUPRA 55VP). To calculate the mean particles sizes of the prepared electrodes, X-ray diffraction (XRD) was performed using a Rigaku Miniflex AD11605 equipped with an X-ray diffractometer and Cu Kα radiation (λ = 1.5405 nm) operated at 30 kV and 30 mA.

MEA fabrication

Carbon-supported Pt catalyst (Johnson Matthey, 40 wt% Pt on carbon black) was used for fuel cell operation. Slurry containing 0.3 g of carbon supported Pt, 1.2 g de-ionized water, 0.8 g of Nafion solution, and 3.6 g of isopropyl alcohol (Aldrich) was mixed and used as catalyst ink. Catalyst slurries were stirred mechanically and ultrasonicated to allow good mixing of the ionomer and Pt nanoparticles. Each step was repeated five times alternately. Catalyst inks were then sprayed onto both sides of the Nafion membranes using an airbrush gun with a catalyst loading of 0.4 mg·cm^{-2}. Both electrodes had an active surface area of 1 cm^2. Then, the catalyst-coated membranes were dried at room temperture for 1 h to remove residual solvent. Single PEMFCs were fabricated by assembly of the catalyst-coated membrane, gas diffusion media (SGL 10BC), and Teflon gasket, without hot-pressing.

Fuel cell characterization

Several electrochemical experiments were carried using single PEMFCs (Fuel Cell Technology, USA). Pure hydrogen and oxygen were fed into the cell as the fuel and oxidation gas, respectively. The flow rates of H_2 and O_2 were 0.1 L·min^{-1} and 0.15 L·min^{-1}, respectively, with a stoichiometry of 1/1.5 (H_2/O_2). Humidification of hydrogen and oxygen was achieved using a bubble humidifier. Feeding reactive gases were preheated to the same temperature as the bubble humidifier. Electrochemical experiments were performed at 75°C and

100% relative humidity (RH) without providing back pressure. A KFM2030 (KIKUSUI) FC impedance meter was used for fuel cell load testing, to determine polarization curves (current density vs. voltage) while a PGSTAT-30 (Autolab) was used for *in situ* EIS and CV measurements. EIS was performed at the same operation conditions to investigate membrane/electrode resistances using an amplitude of 10 mV and a frequency range of 100 mHz–10 kHz. To analyze the catalyst layer, CV scans were performed at the flowrate of H_2 and N_2 were 0.1 $L{\cdot}min^{-1}$ and 0.15 $L{\cdot}min^{-1}$, respectively, in the range of 0.05 to 1.20 V at a scan rate of 50 mV/s.

Conclusions

In summary, we developed a simple, fast, and universal patterning methodology at room temperature based on the control of the interface of MEAs to boost PEMFC performance. Use of a micropatterned Nafion membrane increased the active surface area of the electrode utilization of catalyst and mechanical bonding between the electrode and patterned membrane, resulting in improved electrochemical performance of the MEA. We obtained a 53% improvement in current density and a 59% increase in maximum power density in a PEMFC when using the micropatterned MEA with the highest surface area. Direct patterning of Nafion membranes at even room temperature is scalable to large areas, and is compatible with mass production because the templates used to produce the membrane are easy to use, inexpensive, and reusable, and most importantly, universally applicable to a variety of PEMs. Our approach will facilitate the manufacture of PEMFCs with improved utilization of Pt and a greater electrochemically active electrode surface area than existing PEMFCs. Furthermore, our patterning process can be used to produce a wide variety of patterns and shapes depending on the desired application.

Acknowledgements

We acknowledge the financial support of grants from the National Research Foundation (NRF) funded by the Korean government (MEST) (No. 2009-C1AAA001-2009-0092926) and through the Active Polymer Center for Pattern Integration (R11-2007-050-00000-0).

Notes and references

[a]Department of Chemical and Biomolecular Engineering, Yonsei University, 50 Yonsei-ro, Seodaemun-gu, Seoul 120-749, Korea
‡These authors contributed equally to this work.
* Corresponding authors: E-mail: jonghak@yonsei.ac.kr (Prof. J.H. Kim), shulyg@yonsei.ac.kr (Prof. Y.G. Shul)

Electronic Supplementary Information (ESI) available: Different shapes of the patterns, XRD results and electrochemical performance of the commercial Nafion membrane were shown. See DOI: 10.1039/b000000x/

1. H. Zhang, P. K. Shen, *Chem. Soc. Rev*., 2012, **41**, 2382.
2. T. Miyahara, T. Hayano, S. Matsuno, M. Watanabe, K. Miyatake, *ACS Appl. Mater. Interfaces* 2012, **4**, 2881.
3. C. Xu, Y. Cao, R. Kumar, X. Wu, X. Wang, K. Scott, *J. Mater. Chem*., 2011, **21**, 11359.
4. M.-C. Hsiao, S.-H. Liao, Y.-F. Lin, C.-C. Weng, H. M. Tsai, C.-C. M. Ma, S.-H. Lee, M.-Y. Yena, P.-I. Liu, *Energy Environ. Sci*., 2011, **4**, 543.
5. F. Zhang, Z. Tu, J. Yu, H. Li, C. Huang, H. Zhang, *RSC Adv*., 2013, **3**, 5438.
6. T. B. Norsten, M. D. Guiver, J. Murphy, T. Astill, T. Navessin, S. Holdcroft, B. L. Frankamp, V. M. Rotello, J. Ding, *Adv. Funct. Mater.* 2006, **16**, 1814.
7. X. Li, X. Chen, B. C. Benicewicz, *J. Power Sources* 2013, **243**, 796.
8. D. Fofana, J. Hamelin, P. Benard, *Int. J. Hydrogen Energ.* 2013, **38**, 10050.
9. C. -C. Lin, C. -B. Chang, Y. –Z. Wang, *J. Power Sources* 2013, **223**, 277.
10. Z. Yin, Q. Zheng, *Adv. Energy Mater.* 2012, **2**, 179.
11. Z. Q. Tian, S. H. Lim, C. K. Poh, Z. Tang, Z. Xia, Z. Luo, P. K. Shen, D. Chua, Y. P. Feng, Z. Shen, J. Lin, *Adv. Energy Mater.* 2011, **1**, 1205.
12. H. -S. Oh, H. Kim, *Adv. Funct. Mater.* 2011, **21**, 3954.
13. J. Li, H. Tang, L. Chen, R. Chen, M. Pan, S. P. Jiang, *Chem. Commun.* 2013, **49**, 6537.
14. S. Zhang, Y. Shao, G. Yina, Y. Lin, *J. Mater. Chem. A,* 2013, **1**, 4631
15. K. Schmidt-Rohr, Q. Chen, *Nat. Mater.* 2008, **7**, 75.
16. T. Soboleva, X. Zhao, K. Malek, Z. Xie, T. Navessin, S. Holdcroft, *ACS Appl. Mater. Interfaces* 2010, **2**, 375.
17. Z. Q. Tian, S. P. Jiang, Y. M. Liang, P. K. Shen, *J. Phys. Chem. B* 2006, **110**, 5343.
18. T. Soboleva, K. Malek, Z. Xie, T. Navessin, S. Holdcroft, *ACS Appl. Mater. Interfaces* 2011, **3**, 1827.
19. I. -K. Ding, J. Zhu, W. Cai, S. -J. Moon, N. Cai, P. Wang, S. M. Zakeeruddin, M. Grätzel, M. L. Brongersma, Y. Cui, M. D. McGehee, *Adv. Energy Mater.* 2011, **1**, 52.
20. J. H. Kim, J. K. Koh, B. Kim, J. H. Kim, E. Kim, *Angew. Chem. Int. Ed.* 2012, **124**, 6970.
21. M. Aizawa, H. Gyoten, A. Salah, X. Liu, *J. Electrochem. Soc.* **2010**, **157,** B1844.
22. M. Aizawa, H. Gyoten, *J. Electrochem. Soc.* 2013, **160**, F417.
23. L. Wang, S. G. Advani, A. K. Prasad, *J. Phys. Chem. C* 2013, **117**, 945.
24. W. Song, H. M. Yu, L. X. Hao, Z. L. Ma, B. L. Yi, Z. G. Shao, *Solid State Ionics* 2010, **181**, 453.
25. A. J. Appleby, *J. Electroanal. Chem.* 1993, **357**, 117.
26. M. H. Yildirim, J. Braake, H. C. Aran, D. F. Stamatialis, M. Wessling, *J. Membr. Sci.* 2010, **349**, 231.
27. Z. Zhou, R. N. Dominey, J. P. Rolland, B. W. Maynor, A. A. Pandya, J. M. DeSimone, *J. Am. Chem. Soc.* 2006, **128**, 12963.
28. J. W. Bae, Y. -H. Cho, Y. -E. Sung, K. Shin, J. Y. Jho, *J. Ind. Eng. Chem.* 2012, **18**, 876.
29. A. Omosebi, R. S. Besser, *J. Electroanal. Chem.*, 2011, **158**, D603.
30. A. Omosebi, R. S. Besser, *J. Power Sources* 2013, **228**, 151.
31. A. B. Deshmukh, V. S. Kale, V. M. Dhavale, K. Sreekumar, K. Vijayamohanan, M. V. Shelke, *Electrochem. Comm.* 2010, **12**, 1638.
32. Y. -H. Cho, J. W. Bae, Y. -H. Cho, J. W. Lim, M. Ahn, W. -S. Yoon, N. -H. Kwon, J. Y. Jho, Y. -E. Sung, *Int. J. Hydrogen Energ.* 2010, **35**, 10452.
33. Y. Qiao, C. M. Li, *J. Mater. Chem.,* 2011, **21**, 4027.
34. S. Chen, Z. Wei, H. Lib, L. Li, *Chem. Commun* 2010, **46**, 8782.

35. M. Uchida, Y. -C. Park, K. Kakinuma, H. Yano, D. A. Tryk, T. Kamino, H. Uchida, M. Watanabe, *Phys. Chem. Chem. Phys.* 2013, **15**, 11236.
36. S. S. J. Aravind, S. Ramaprabhu, *ACS Appl. Mater. Interfaces* 2012, **4**, 3805.
37. D. Zhao, B. -Q. Xu, *Angew. Chem. Int. Ed.* 2006, **118**, 5077.
38. K. Karan, *Electrochem. Commun.* 2007, **9**, 747.
39. W. Zhua, D. Kub, J. P. Zheng, Z. Liang, B. Wang, C. Zhang, S. Walsh, G. Auf, E. Plicht, J. *Electrochim. Acta* 2010, **55**, 2555.
40. T. Yuan, H. Zhang, Z. Zou, S. Khatun, D. Akins, Y. Adam, S. Suarez, *Membranes* 2012, **2**, 841.
41. S. Wang, G. Sun, Z. Wu, Q. Xin, *J. Power Sources* 2007, **165**, 128.

Table of Contents/Abstract Graphic

We report a facile universal patterning method that provides a large electrochemical area and well-arrayed patterns of polymer electrolyte membranes at low cost using an elastomeric mold at room temperature without hot-pressing. The membrane electrode assembly (MEA) fabricated with 3 × 5 μm (width × gap) patterned Nafion membrane exhibited a high current density of 1.79 A/cm^{-2} at 0.6 V, which was approximately 52.9% greater than that of the MEA without a pattern.